Experimental Thermal and Fluid Science 109 (2019) 109884

Contents lists available at ScienceDirect

Experimental Thermal and Fluid Science

journal homepage: www.elsevier.com/locate/etfs

Aerodynamics loads variations of wings with novel heating of top surface: Bioinspiration and experimental study

M. Hassanalian[a,*], V. Pellerito[a,b], A. Sedaghat[c], F. Sabri[c], L. Borvayeh[d], S. Sadeghi[c]

[a] Department of Mechanical Engineering, New Mexico Tech, Socorro, NM 87801, USA
[b] Department of Mechanical Engineering, Lawrence Technological University, Southfield, MI 48075, USA
[c] Department of Mechanical Engineering, Australian College of Kuwait, Kuwait
[d] Department of Mathematics, Australian College of Kuwait, Kuwait

ARTICLE INFO

Keywords:
Heated boundary layer
Surface temperature
Aerodynamic loads
Drones
Efficiency

ABSTRACT

Applications of unmanned aerial vehicles are becoming more attainable through the increase in system efficiency. As seen in nature, birds like the albatross utilize the temperature effects resulting from their wings' color to increase their flight efficiency. In this paper, the effects that differences in surface temperatures of birds' black/white wings, colored flat plates, and airfoils with heating films is investigated. Such effects are applicable to the efficiency of fixed-wing drones. Experimentally, it is observed that the surface temperature of black birds' wings is over 50% higher than white wings under solar radiation. The application of a novel heated top surface on five airfoils results in the drag coefficient decreasing up to 60% and the lift coefficient increasing up to 70% for some airfoils in specified angles of attack compared to a non-heated top surface. This method of utilizing thermal effects can be considered as a new applicable way to increase the flight efficiency in fixed-wing unmanned aerial vehicles.

1. Introduction

In recent decades, there has been a tremendous effort in the design of drones. As technologies advance, the need for high-performance drones with a magnitude of capabilities including unmanned, micro, and nano air vehicles has increased for both civilian and military applications [1]. This introduces a new era in which autonomous unmanned aerial vehicles are capable of perceiving and generating solutions in complex environments [2,3]. Drones' benefits include the potential to carry out a variety of operations including: reconnaissance, patrolling, protection, transportation of loads, and aerology [4]. Due to their several potential applications and functions, the popularity of these devices has greatly risen, leading to a variety of unique drones with different sizes, shapes, and weights [1,4]. Moreover, the development in micro-electro-mechanical systems (MEMS), sensors, fabrication and navigation methods, and power systems have made the design and manufacturing of a wide range of drones possible [1]. In other words, drones often vary widely in their configurations depending on the platform and mission. Therefore, there are various classifications for them based on different parameters [1].

Considerable advantages of drones have led to the conduction of a myriad of studies aiming to optimize and enhance the ability of this group of planes [5]. To this end, several research studies from distinct disciplines (mechanical, aerospace, material, electrical, computer science, etc.) have focused on the design, optimization, and performance enhancement of drones which resulted in the development and fabrication of various types of these unmanned systems. Most relevantly, in the past decade, there has been a push to design and fabricate drones which can accomplish high endurance missions at optimal performance [1,6].

With the present energy crisis, there is an ever-increasing need for research in performance enhancement techniques. Since nature has developed objects, processes, materials, and the functions to increase efficiency, it has the best answers when we seek to improve or optimize a system. Thus, the fields of biomimetics and bioinspiration allow us to mimic avian to develop methods for reducing drag in all types of transportations in air and water [7,8]. Avian flight can be considered as very efficient flying machines; thus, bio-inspired designs offer potential benefits for drones [3]. Inspired from natural flyers, the evolution of unmanned aerial vehicles has advanced drastically over the past few years, and due to the birds' flight capabilities, they are an ideal study subject to base the design of drones upon. Based upon the research witnessed in migrating birds, engineers have worked on developing similar capabilities in drones in order to improve their endurance,

* Corresponding author.
E-mail address: mostafa.hassanalian@nmt.edu (M. Hassanalian).

https://doi.org/10.1016/j.expthermflusci.2019.109884
Received 2 July 2019; Received in revised form 26 July 2019; Accepted 28 July 2019
Available online 29 July 2019
0894-1777/ Published by Elsevier Inc.

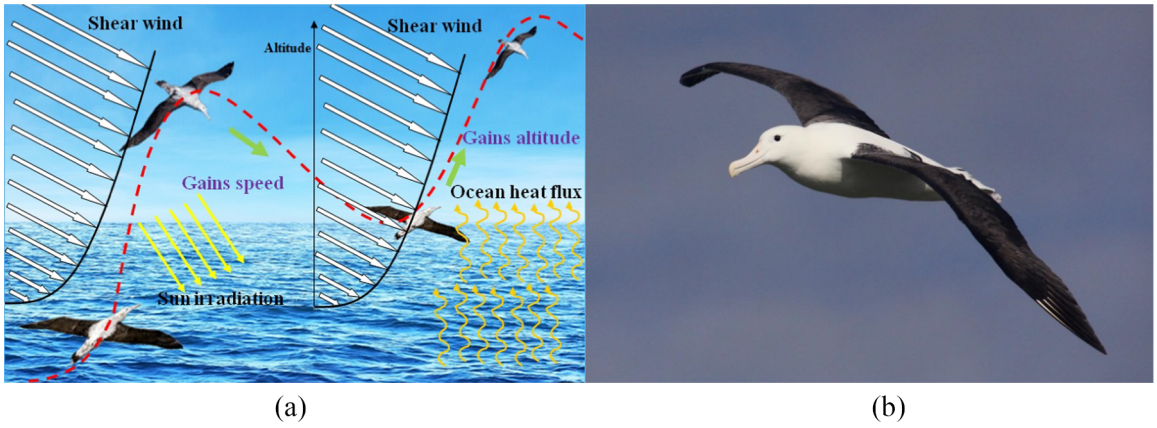

Fig. 1. View of (a) albatross dynamic soaring and (b) top wing black color.

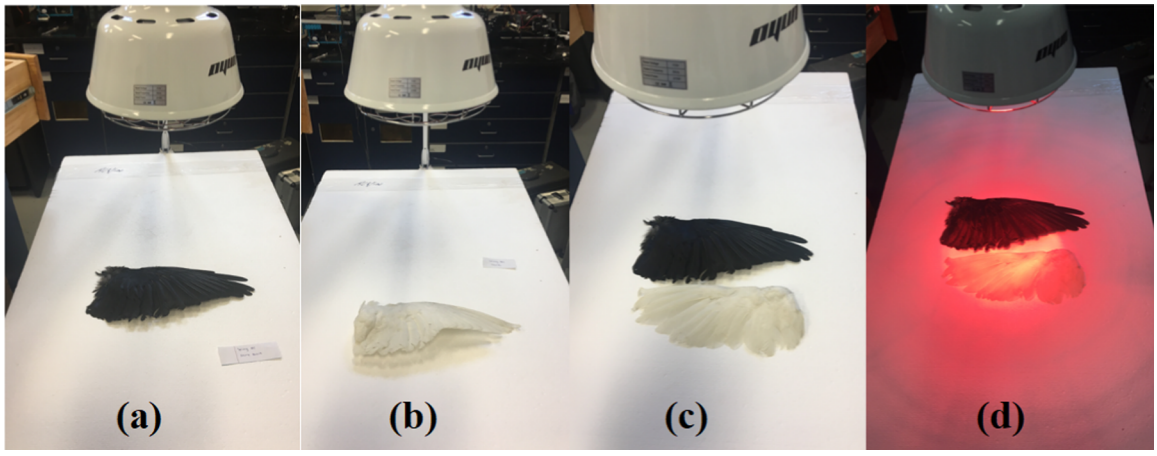

Fig. 2. Views of the designed experimental setup; (a) black wing, (b) white wing, (c) black and white wings, and (d) black and white wings under the radiation of the heat lamp.

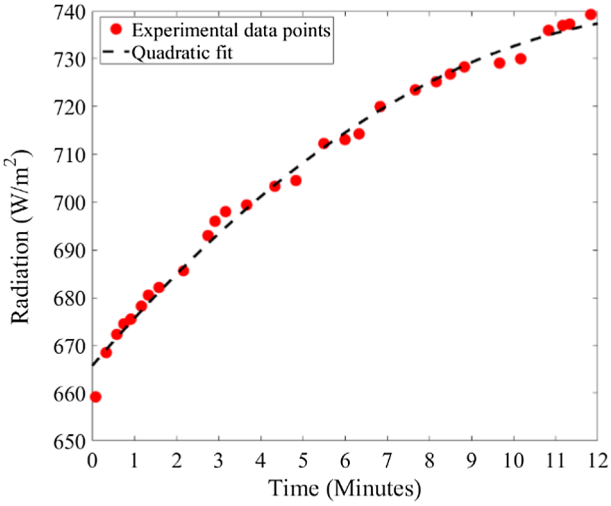

Fig. 3. Radiation versus time for heat lamp with 40 cm distance from the plate.

altitude, velocity, maneuverability, compressibility, stealth, and/or payload [3]. To this end, several bio-inspired designs have helped to improve upon drones' speed, endurance, efficiency, and maneuverability.

It was investigated by Hassanalian et al. [9,10] that the black and white colors of migrating birds' wings, such as albatrosses, shearwaters, sooty terns, and black skimmers have an effect on their skin drag reduction [9–11]. In this study, the migration routes of birds with black and white colors, including the latitudes and longitudes, the time of migration, and the corresponding marine and atmospheric characteristics such as wind speed, ambient temperature, ocean temperature, and sky temperature of their flight routes were extracted [9]. The thermal effects of top and bottom sides of the wing with two different colors (white and black) were studied. Using Blasius boundary condition, it was shown that the boundary layer around the wings of the birds with black color on top have less density and more viscosity than white color [9]. In other words, for the dark colors, there is an increase in the wing surface temperature and therefore a corresponding decrease in the density and an increase in the viscosity, but the total skin drag decreases.

Generally, the effects of temperature have been studied experimentally and numerically on both laminar and turbulent boundary layers for a long time [12–17]. Various tests have been performed on low-speed and long-chord airfoils for de-icing of the airplanes' wings [18]. It has been shown that there are considerable effects on lift and drag performance of the wings with a heated leading edge [19]. The Reynolds number changes inversely with the temperature of the flow and decreases as the temperature increases. Generally, for laminar flow, with increasing the temperature the local Reynolds number and the corresponding wall shear stress and skin friction drag decrease. Dragan investigated the thermal effects on the performance of a NACA 2510 airfoil [19]. In this study, the NACA 2510 airfoil with adiabatic walls and the same airfoil with heated patches were compared and it was indicated that surface temperature distribution influences the aerodynamics of an airfoil [19].

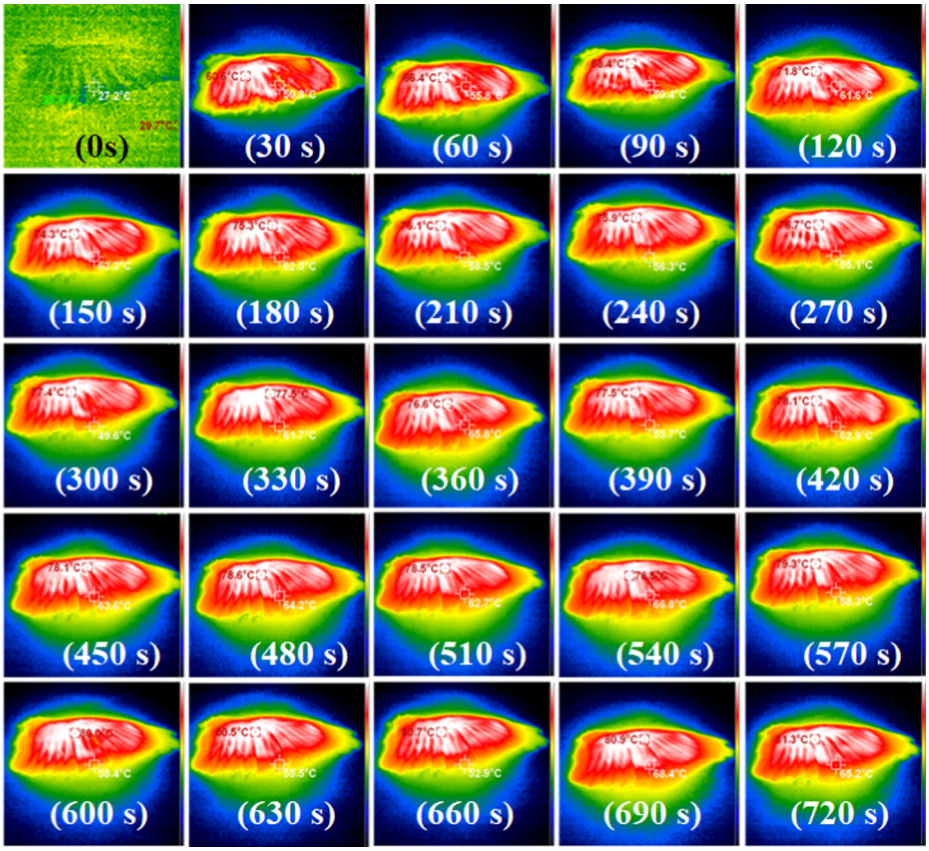

Fig. 4. Thermal images of a black wing under the heat lamp in 30-second intervals.

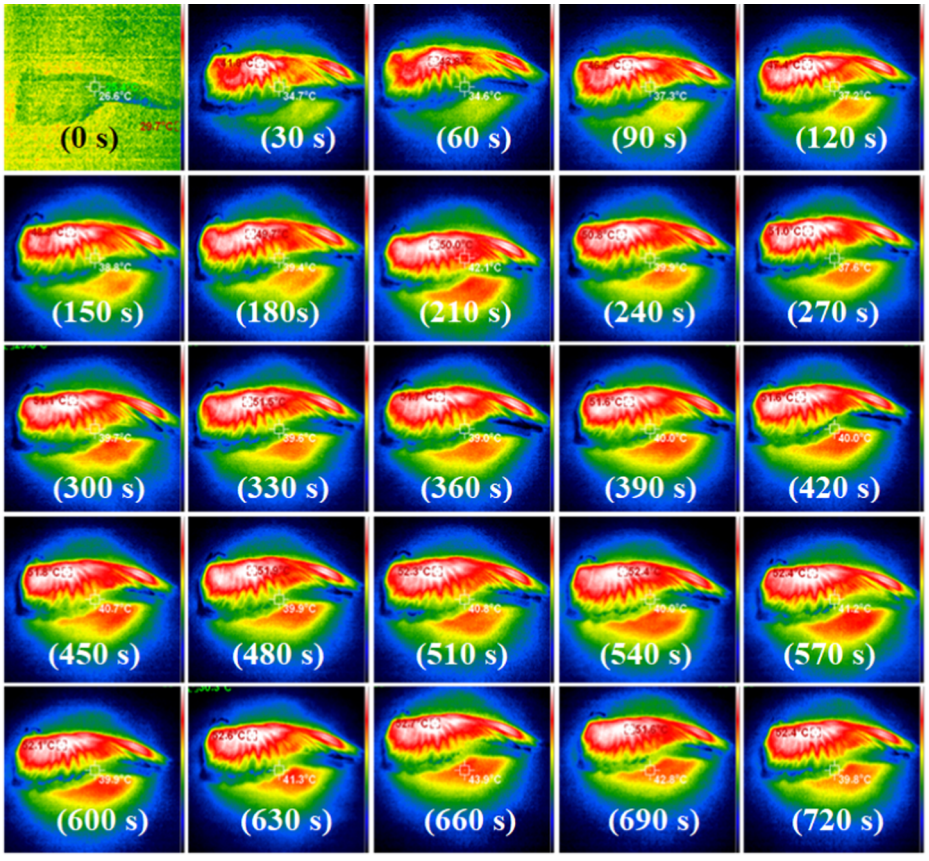

Fig. 5. Thermal images of a white wing under the heat lamp in 30-second intervals.

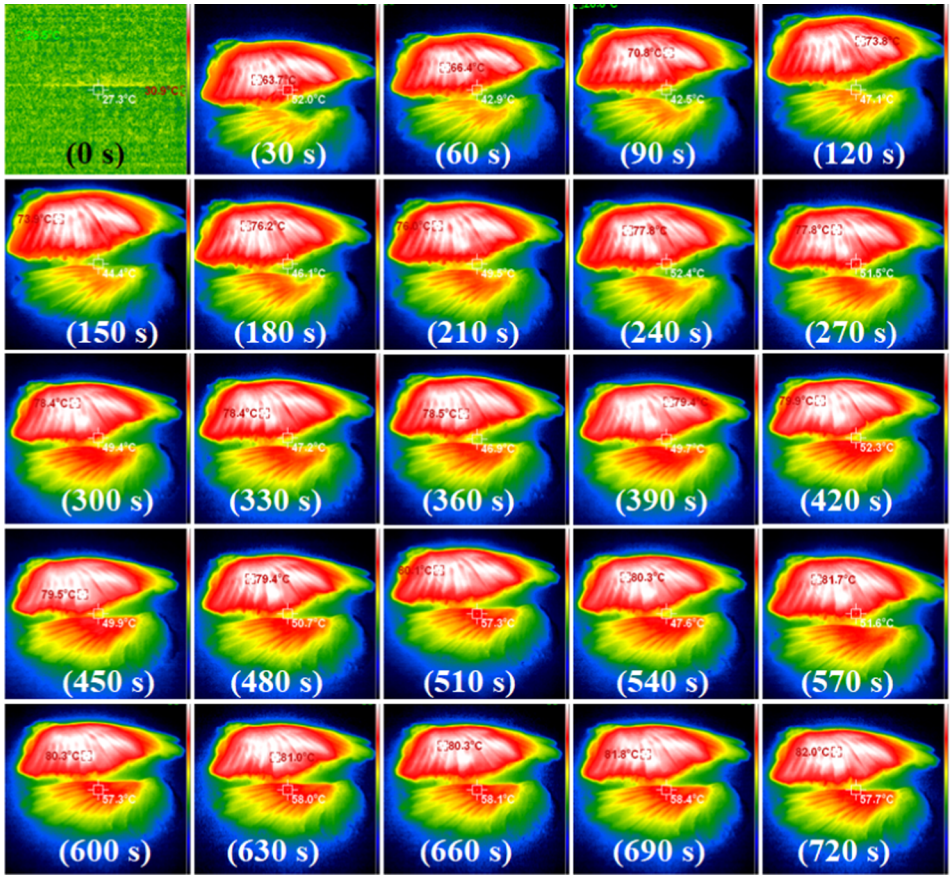

Fig. 6. Thermal images of black (top) and white (bottom) wings in 30-second interval.

It should be noted that mechanisms of drag reduction in ocean-migrating birds are opening a new bioinspired performance enhancement technique which is called the heated boundary layer. To this end, in this paper, a novel mechanism for fixed-wing drones that provides a heated boundary layer of air over the top part of its wing is proposed. This is accomplished through applying a heated blanket and temperature controller on the top part of the drone's wing. This concept will be able to increase the performance of fixed-wing drones by increasing the lift and decreasing the drag forces. This paper reviews the geometric and flight characteristics of albatrosses in Section 2. In Section 3, the energy balance and governing equations for albatrosses are presented. Experimental study on the effects of colors on the surface temperature of birds' wings and aluminum plates are shown in Sections 4 and 5, respectively. The experimental study of the effect of a heated surface for different airfoils is discussed in Section 6. Summary and conclusions are given in Section 7.

2. Geometric and flight characteristics of albatrosses

Generally, birds have different flight modes which can be divided into two modes, namely, powered fight (hovering and flapping flights) and unpowered flight (soaring and gliding Flights). Some types of migrating birds like albatrosses can fly long-distance trips of 15200 km over the ocean without any flapping motion during 46 days [20,21]. These large migrating birds fly most of their lives over the oceans and return to small oceanic islands only for breeding [22]. Albatrosses which have a wingspan of 3.5 m and weight of 8.5 kg are able to fly with maximum ground speeds of over 35 m/s [23]. These birds can also maintain these speeds for more than 8 h without any flapping motion [24]. Assuming a maximum lift to drag ratio of 20, an albatross need a power of 81 W for flying at 19.5 m/s [25].

Different theories have been proposed by researchers to explain how these migrating birds can fly without flapping and just extending their wings. These birds due to their anatomical adaptations have an elbow-lock system and without any muscle activity can keep their wing open [25]. The main theory behind their long and low-cost flight is their special flight mode, which is called dynamic soaring. Albatrosses are able to take advantage of wind shear to gain the required energy for flying. These migrating birds increase their height above the ocean surface and apply the wind speed to gain energy. Also, they can use updrafts caused by wind blowing over waves to gain energy which is called wave-slope soaring. It should be noted that wind blowing over the ocean waves has both wind shear and vertical motions that influence each other [10]. Albatrosses generally have two types of movement in different scales; one is a large-scale movement that appears as a steady-state cruise of long-distance flight and next is small scale movement which is flight maneuvers of highly dynamic nature. The large scale movements are of the order of hundreds to thousands of kilometers, and the small-scale movements are of the order of tens to hundreds of meters constituting dynamic soaring [26].

Albatrosses as ocean migrating birds have black and white colors. The concentration of melanin in top feathers of these migrating birds causing the wings to appear black on top. As discussed before, these birds have drag reduction due to the heated boundary layer on the top of their wings. In Fig. 1(a) and (b), views of dynamic soaring and colors of the wings of an albatross are shown, respectively.

3. Energy balance and governing equations for albatrosses

It is obvious that the heat absorption of dark-colored objects is greater than lighter colored objects. Considering this heat transfer principle, it was indicated computationally by Hassanalian et al., that the top surface of the albatross's wings has a higher temperature once they are exposed to the sun radiation due to their black color [10]. To

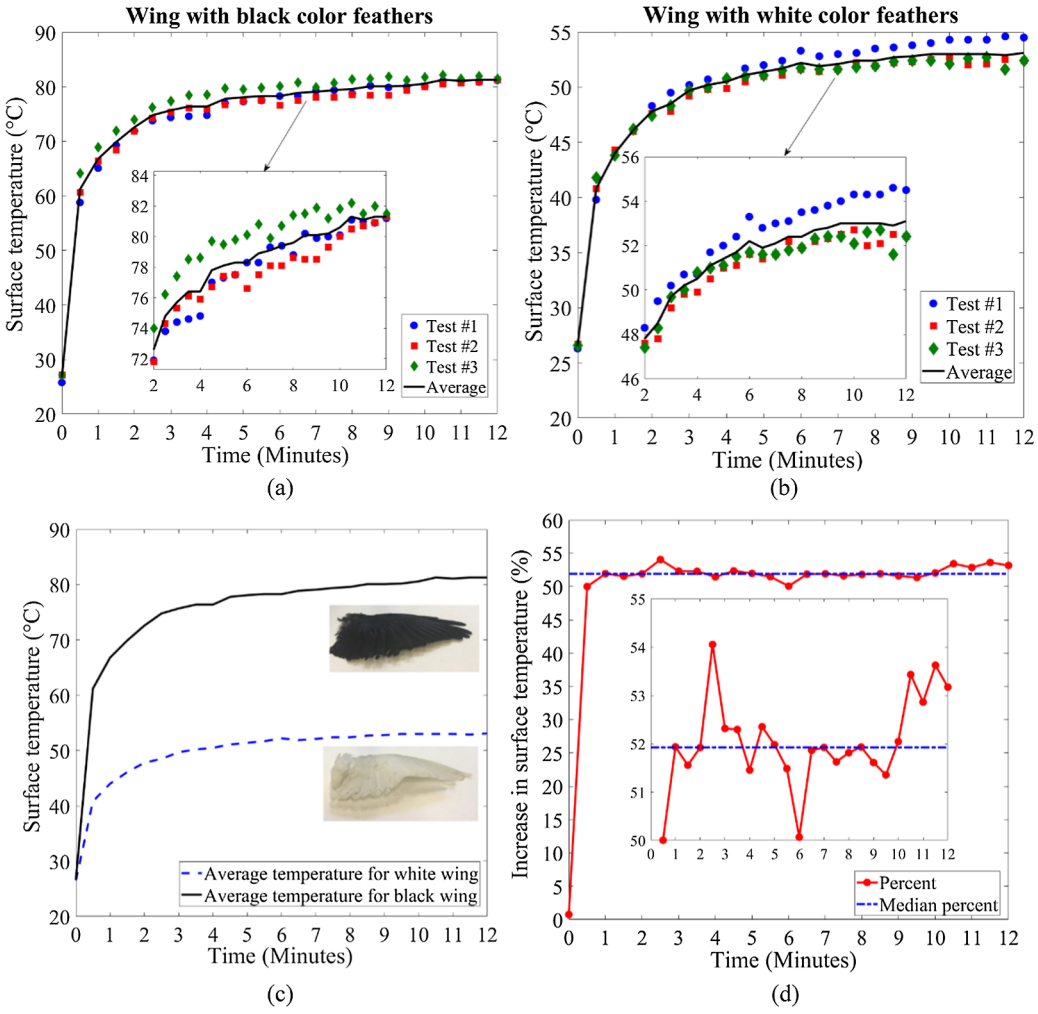

Fig. 7. Views of (a) surface temperature for the black color wing, (b) surface temperature for the white color wing, (c) comparison of surface temperatures for the wings with black and white colors, and (d) percentage of increase in surface temperature for black wing compared to the white wing.

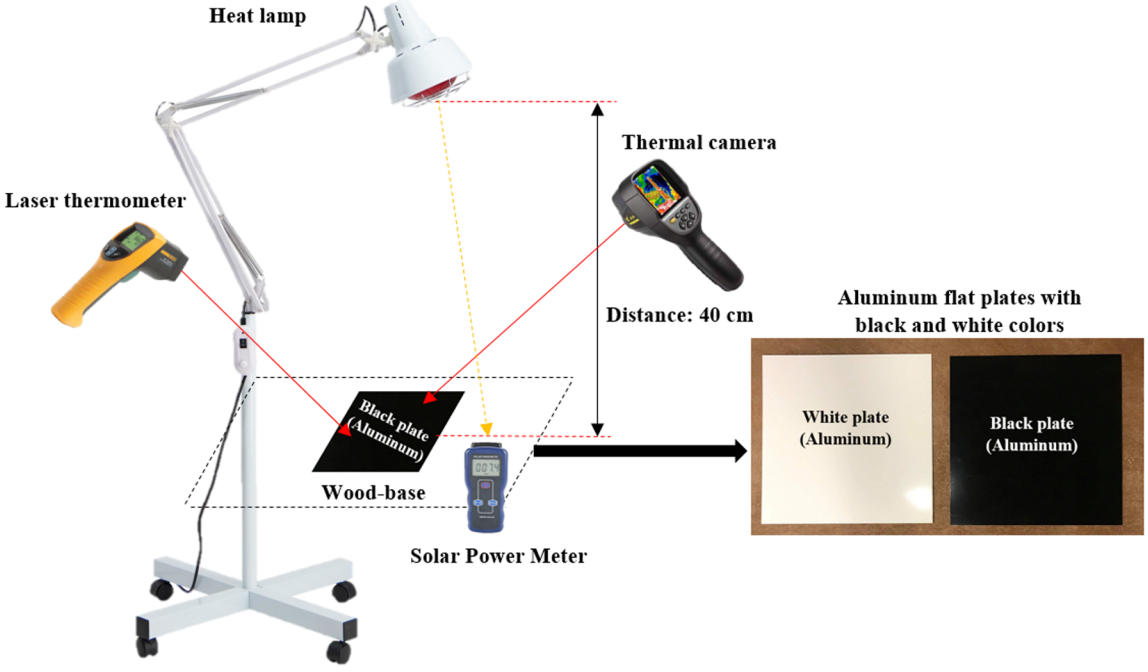

Fig. 8. Experimental setup to study the color effects on the surface temperature of aluminum flat plates.

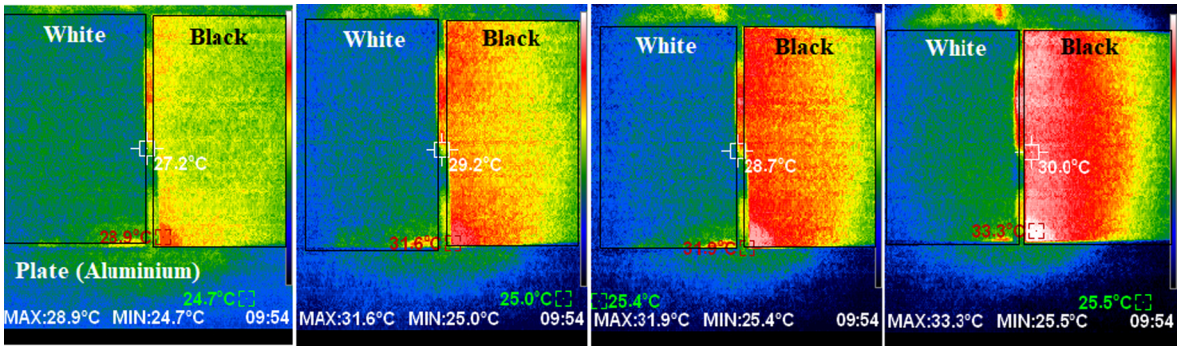

Fig. 9. Surface temperature distribution for black and white aluminum plates.

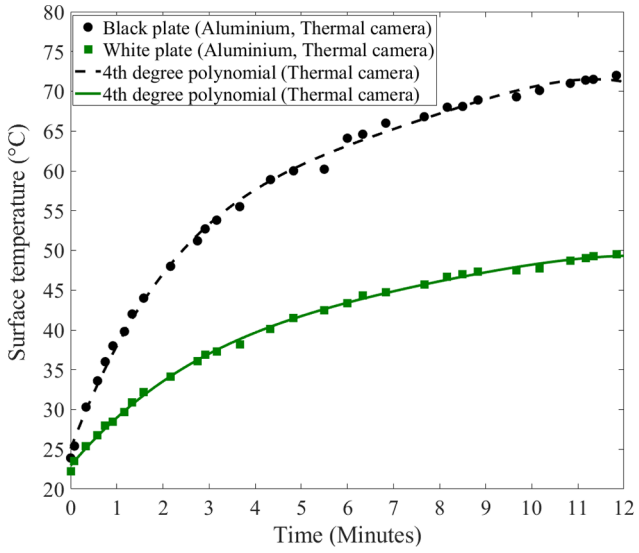

Fig. 10. Surface temperature versus time for white and black aluminum plates.

Table 1
Geometric characteristics of the studied airfoils.

Airfoil	Max. thickness (%)	Max. thickness @ (%)	Max. camber (%)	Max. camber @ (%)
NACA 2412	12	29	2.00	40
GOE 174	8.58	20	5.57	40
S5020	8.40	28	2.62	28
E186	10.27	31	1.31	27
MH20	9	33	2.04	37

this end, they conducted research on thermal effects of the color of the albatross's wings in their flight performance. In their research, they assumed that when the heat reaches the surface of these migrating birds, a portion is absorbed, another is reflected, and the rest is transmitted. Since the wings are considered as opaque surfaces, the transmitted portion was neglected. Considering the wing as a flat plate, an energy balance equation was written for the top part of the albatross wing as follows [9,10]:

$$\alpha_s G_s + \alpha_{sky} G_{atm} = h(T_S - T_\infty) + \varepsilon\sigma T_S^4 \quad (1)$$

where α_s, α_{sky}, ε, σ, G_s, G_{atm}, h, T_S, and T_∞ are solar absorptivity of surface and sky, emissivity of surface, Stefan–Boltzmann constant, solar irradiation, irradiation at the earth's surface due to atmospheric emission, convective heat transfer coefficient, and surface and environment temperatures, respectively [9]. It has been assumed that the absorptivity of the sky is almost equal to the emissivity of the surface ($\alpha_{sky} \approx \varepsilon$) and the irradiation at the earth's surface due to atmospheric emission is $G_{atm} = \sigma T_{sky}^4$, where T_{sky} is the effective sky temperature, the energy balance finally has been written as [9,10]:

$$\alpha_s G_s = h(T_S - T_\infty) + \varepsilon\sigma(T_S^4 - T_{sky}^4) \quad (2)$$

Solving the above energy balance, it has been shown that the temperature difference between the bright and dark-colored top wing surface is around 10 °C for a flat plate [9]. Finally, considering the effects of the temperature on the viscosity and the density of the air, the skin drag force was calculated in different seasons. It follows from the primary results performed by Hassanalian et al. [9,10], that a dark-colored wing generates less drag than a white-colored one for different seasons. This means that for the albatross, its black top wings are helping it to improve its flight performance by reducing the drag force. Since the previous study by Hassanalian et al. [9,10] is lack of experiment, in this study with inspiration from albatross wing color, some experimental tests in a wind tunnel are carried-out by heating the top surface of wings with different airfoils including the albatross airfoil, GOE-174.

4. Experimental study on effects of feathers' colors on surface temperature of birds

To investigate the surface temperatures of different wing colors two wings, one black and one white, of similar size and shape are placed under a heat lamp. The heat lamp is located 40 cm above the Styrofoam surface that the wings are placed on, simulating sun irradiation. The two wings are exposed to the heat lamp for 12 min, and their surface temperatures are measured by a thermal camera every 30 s. To measure the radiation of the heat lamp, a SM206 Digital Solar Power Meter Sun Light Radiation Measuring Testing Instrument is used. In Fig. 2, the designed experimental setup and the black and white wings are shown.

In Fig. 3, a view of measured radiation of the heat lamp with the Solar Power Meter is shown. The results show that with increasing the time, the radiation of the heat lamp increases.

Various tests are performed on the black and white color wings. In Figs. 4 and 5, the thermal images of the black and white wings at 30 s intervals are shown, respectively. In Fig. 6, the thermal images of a black and white wings at 30 s intervals shows the temperature distribution of the black and white wing together. These images show the contrast in temperature distributions among the black and white wings.

The maximum temperatures over time for three tests of the black and white wings are plotted in Fig. 7(a) and (b), respectively, based on the recorded temperature from the thermal camera. The averages of the black and white wings are compared in Fig. 7(c). The maximum average surface temperature reached for the black and white wings are 81.3 °C and 53.1 °C, respectively. The median percent increase in surface temperature from the white wing to the black wing is 52%, as noted in Fig. 9 (d). The results show that birds' wings with black and white colors can have different surface temperature once they are exposed to sun radiation.

Fig. 11. Views of studied airfoils and wings.

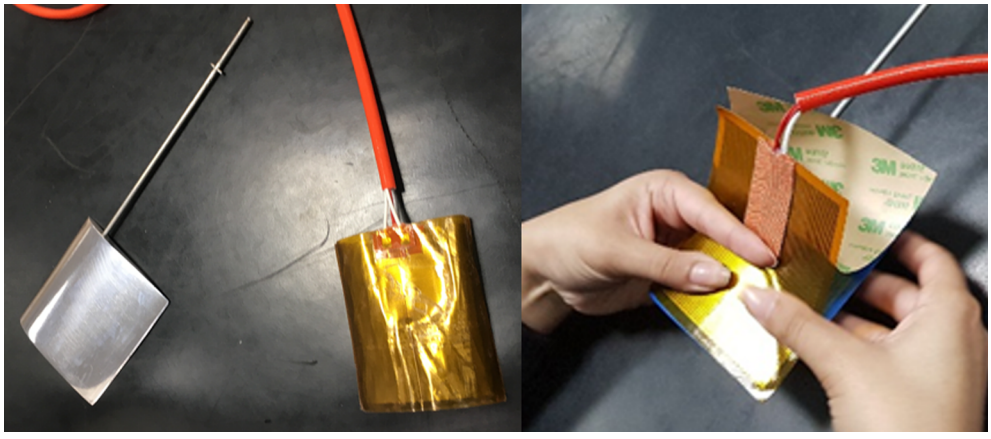

Fig. 12. Views of the aluminum wing and heating film on the top surface of the wing.

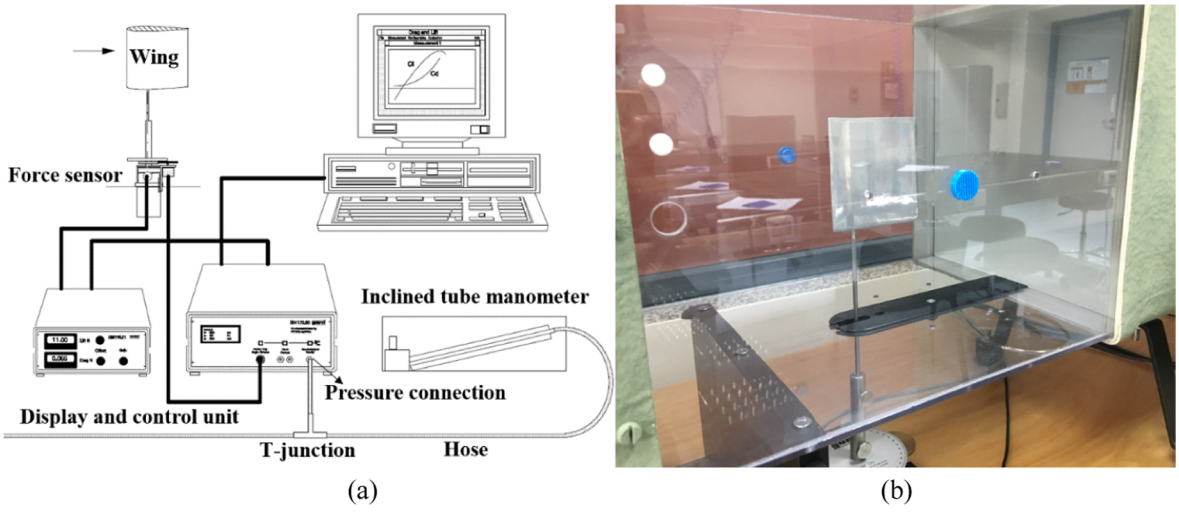

Fig. 13. (a) Schematic view of Educational Wind Tunnel HM 170, and (b) designed experiment for wind tunnel testing.

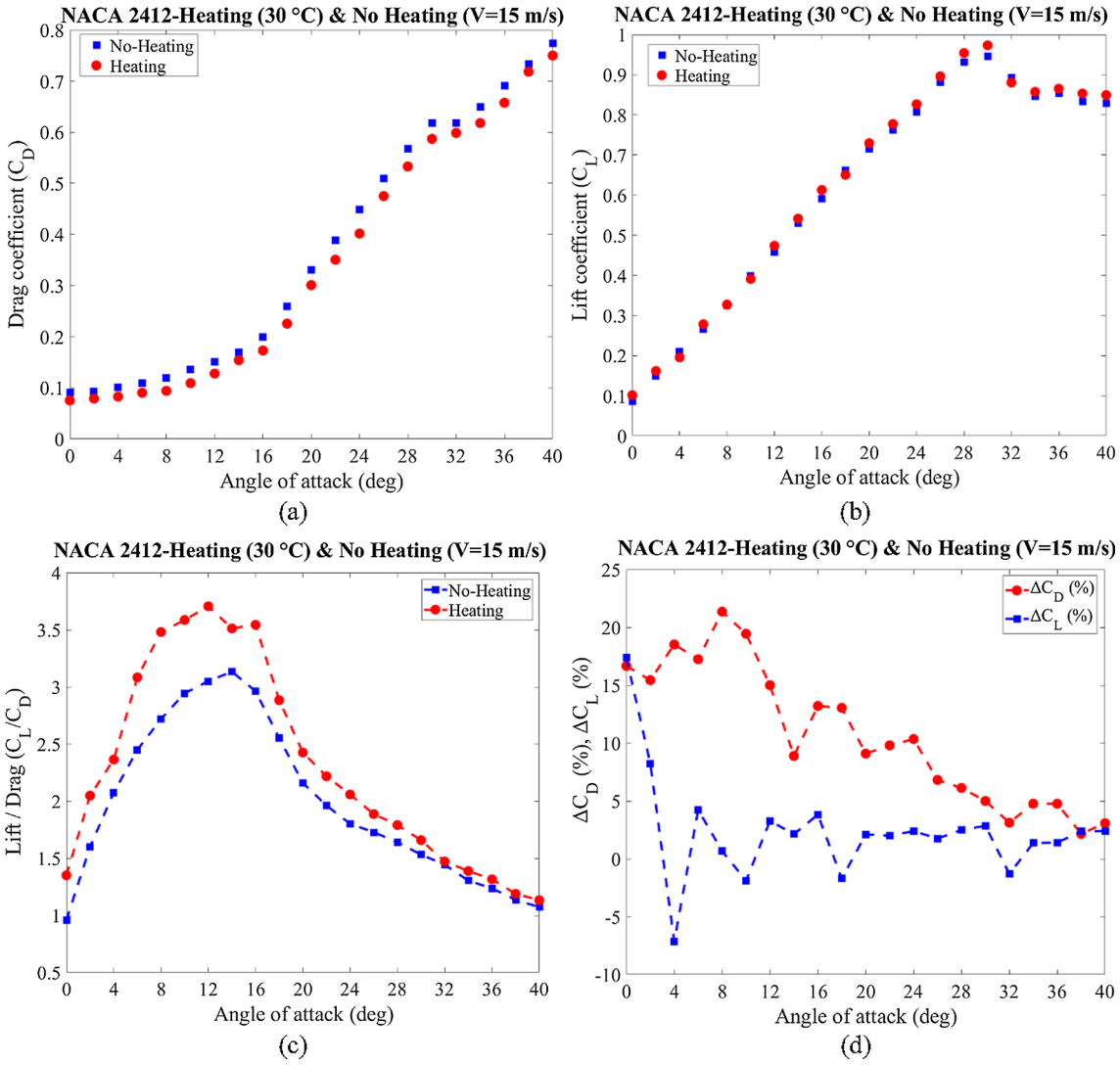

Fig. 14. View of (a) drag coefficient, (b) lift coefficient, (c) lift to drag, and (d) relative changes (percentages) of the lift and drag coefficients versus angle of attack of NACA 2412 for heating and no heating conditions in the wind speed of 15 m/s.

5. Experimental study on effects of color on surface temperature of aluminum plates

To study the effects of the colors on the surface temperature of flat plates with black and white colors, a static experiment is set up in the laboratory. In this experiment, the surface temperature of two black and white aluminum flat plates is measured under a heat lamp. The heat lamp has the same distance of 40 cm from the plates similar to previous experiment carried-out on birds' wings. The two aluminum plates are exposed to the heat lamp for 12 min, and their surface temperatures are measured by a thermal camera and laser thermometer. In Fig. 8, the designed experimental setup and the black and white flat plates are shown. It should be noted that the experiments are conducted in a wood-base material to decrease the conductivity effects.

In Fig. 9, the surface temperature distribution is shown for the aluminum flat plates with white and black colors. It is indicated by a thermal imaging camera that for a similar value of the radiation in this experiment, different surface temperatures can be recorded for white and black color plates. As can be seen in Fig. 9, the results demonstrate higher values of surface temperature for black colored flat plate compared to white-colored due to its higher value of solar absorptivity. The dark and white colors have a solar absorptivity of 0.97 and 0.21, respectively. The same trend was seen in Section 4 for the feathers of the birds with black and white color.

Fig. 10 demonstrates the comparison of surface temperature for the wood-base white and black aluminum plates. It is apparent from Fig. 10 that a maximum temperature difference of almost 22 °C can be found between white and black colored aluminum plates.

As can be seen in Figs. 7(c) and 10, the surface temperature for both black and white colors wings are higher than the surface temperature of the aluminum flat plate with black and white colors, respectively. The main reason for this difference in surface temperature is the value of the conductivity coefficient for the aluminum flat plate and the feathers. The results indicate that feathers can have higher values of the surface temperatures.

6. Experimental study on wings with a heated top surface

In this experimental study, the airfoil of the Wandering albatross (Diomedea exulans) as one of the largest migrating seabird and four other airfoils are taken into consideration. To this end, GOE 174 as well-defined geometric airfoil for albatross, and NACA 2412, GOE 174,

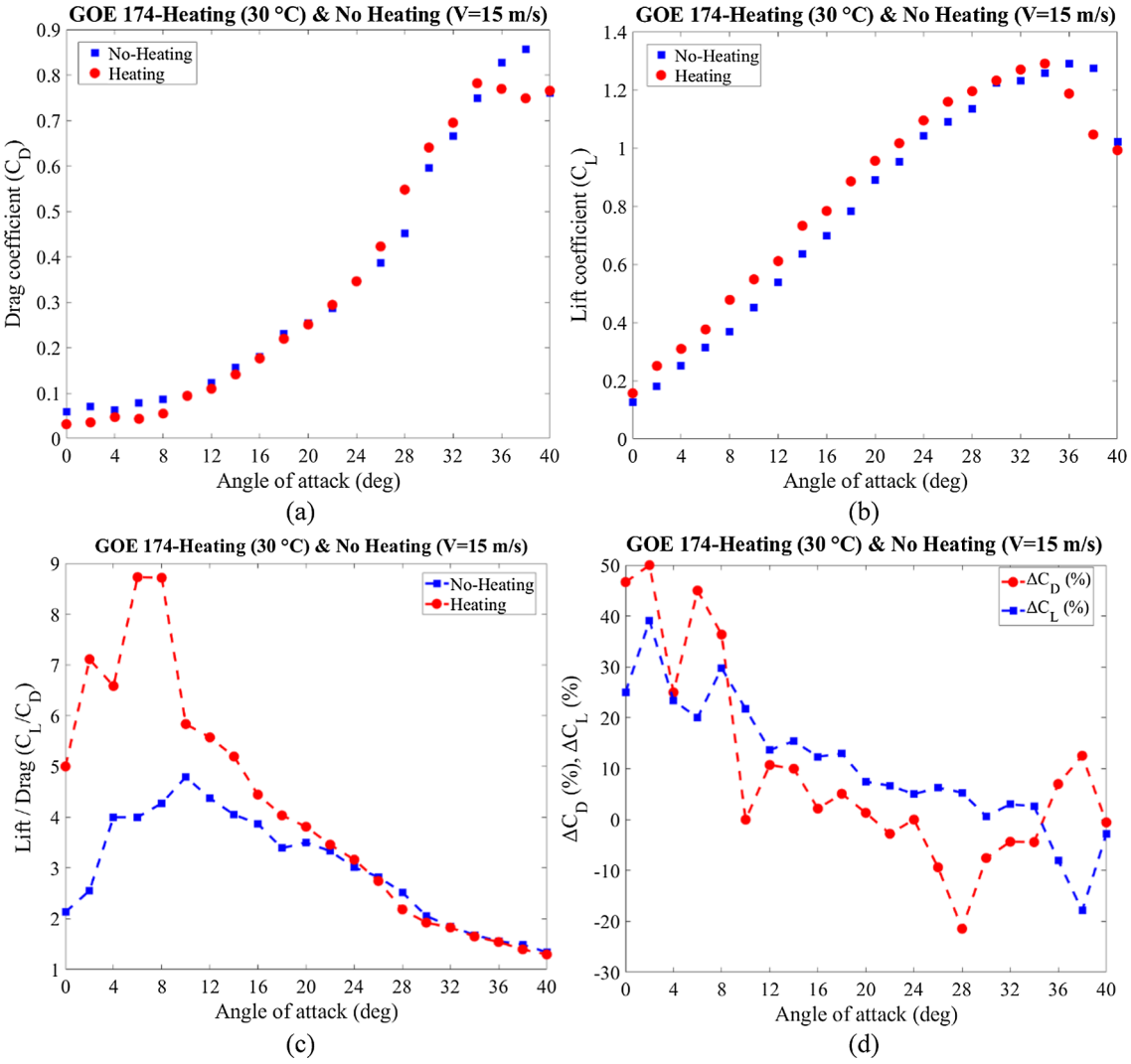

Fig. 15. View of (a) drag coefficient, (b) lift coefficient, (c) lift to drag, and (d) relative changes (percentages) of the lift and drag coefficients versus angle of attack of GOE 174 for heating and no heating conditions in the wind speed of 15 m/s.

S5020, E186, and MH20 are selected. The characteristics of the considered airfoils are shown in Table 1. As can be seen in Fig. 11 different types of reflexed and non-reflexed airfoils are tested in this study.

For all considered airfoils in this study, a wingspan of 100 mm and a chord length of 100 mm is produced using aluminum cast (see Fig. 11).

A heating blanket with a thickness of 0.5 mm with an input power of 75 W is designed using silicone heating film and attached with a digital temperature controller to the wings (see Fig. 12). For the working temperature of 20 ˚C in the wind tunnel, the top surface of the wing is covered with a heating blanket and is tested at different angles of attack at a speed of 15 m/s.

All the manufactured wings with mentioned airfoils are tested in the Educational Wind Tunnel HM 170. In Fig. 13(a) and (b), a schematic view of the wind tunnel and the designed experiment for wind tunnel testing are shown, respectively. In this experiment, the aerodynamic forces of drag and lift are measured for all of the considered wings with top part heated and not heated.

In this experiment, the ambient temperature of the wind tunnel is 20 ˚C and the temperature of the top wing surface is set to 30 ˚C in the case of the heating. The experiments are carried out for all the wings with top heating and no heating conditions. In other words, a temperature difference of 10 ˚C is created for the top part of the wing, which is similar to the difference between the white and dark-colored top wing surface of albatross calculated by Hassanalian et al. [6,7]. The aerodynamic coefficients of lift and drag are measured based on the classical aerodynamic theories as follows.

$$C_L = \frac{2L}{\rho V^2 S} \tag{3}$$

$$C_D = \frac{2D}{\rho V^2 S} \tag{4}$$

where L and D are lift and drag forces measured through the experiment carried out in wind tunnel, ρ is the air density, V is the velocity, and S is the wing area. Experimental results for the lift and drag coefficients, lift to drag ratio, and the relative changes (percentages) of the lift and drag coefficients versus angle of attack for heating and no heating conditions at a wind speed of 15 m/s are obtained for all considered airfoils. The results are shown in Figs. 14–18 for NACA 2412, GOE 174, S5020, E186, and MH20, respectively in different angles of attack. It should be noted that in Figs. 14(d)–18(d), ΔC_D and ΔC_L indicate the drag reduction and lift enhancement percentages.

The results in Fig. 14(a) demonstrate that for NACA 2412 the drag coefficient is decreasing for all angles of attack in a top heated

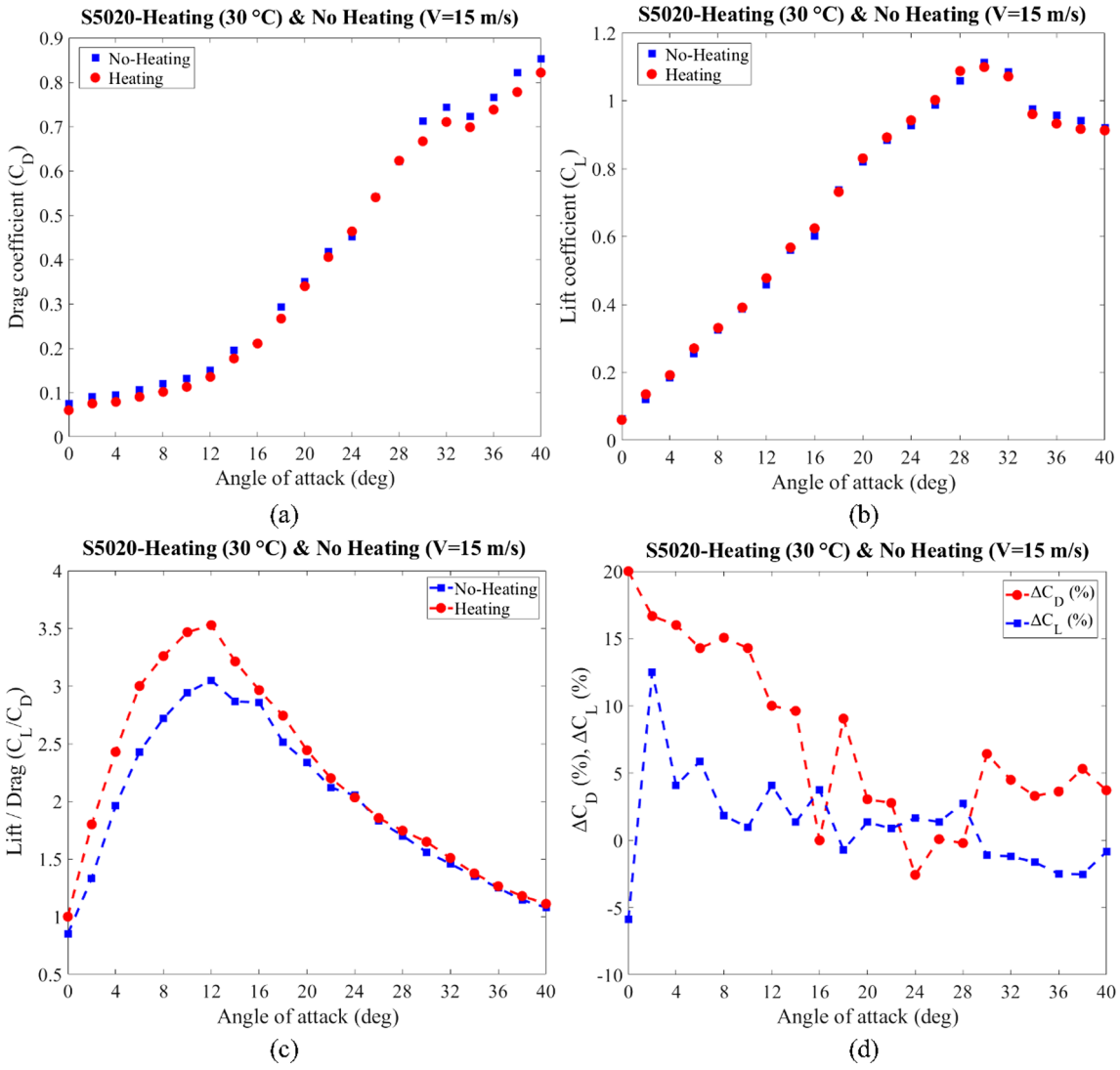

Fig. 16. View of (a) drag coefficient, (b) lift coefficient, (c) lift to drag, and (d) relative changes (percentages) of the lift and drag coefficients versus angle of attack of S5020 for heating and no heating conditions in the wind speed of 15 m/s.

condition. Fig. 14(b) indicates that the lift coefficient for the heating wing increases for most angles of attack. The lift to drag ratio increases for all angles of attack for the top-heated wing (see Fig. 14(c)). It can be seen in Fig. 14(d) that relative changes of drag coefficient decrease in some angles of attack up to 22% and relative changes of lift coefficient increase up to 17%.

Fig. 15(a) shows that for bioinspired albatross airfoil (GOE 174), the drag coefficient is decreasing with increasing the top surface temperature for the angles of attack less than 20 degrees. Fig. 15(b) demonstrates that the lift coefficient for the top-heated wing increases until an angle of attack of 34 degrees. The experimental results in Fig. 15(c) shows that the lift to drag ratio increases for angles of attack up to 24 degrees and the maximum value of the lift to drag ratio can be achieved in angles of attack of 6 to 8 degree. Fig. 15(d) indicates that relative changes of drag and lift coefficients decrease with increasing the angle of attack and the maximum values can be seen in angles of attack of 0 to 2 degree. It is apparent from Fig. 15(d) that a drag reduction of 50% and lift enhancement of 40% can be obtained for a top-heated wing at an angle of attack of 2 degrees.

The wind tunnel results indicate that for a top-heated wing with a reflexed airfoil of S5020 the drag coefficient is decreasing for almost all the angles of attack (see Fig. 16(a)). Fig. 16(b) shows that the lift coefficient increases for the angles of attack up to the stall angle and decreases for angles higher than the stall angle. As can be investigated from Fig. 16(c), the lift to drag ratio increases for all the angles of attack and this ratio has higher values for the angles less than the stall angle and for the angles of attack more than 22 degrees, there is a slight change in the lift to drag ratio. For S5020, a maximum drag reduction of 20% and lift enhancement of 12.5% can be seen in angles of attack of 0 and 2 degrees, respectively (see Fig. 16(d)). The changes in drag reduction and lift enhancement are almost positive for most of the angles of attack.

As can be seen in Fig. 17(a) and (b), respectively, drag coefficient values decrease for the top-heated wing with the E186 airfoil for angles of attack up to 12 degree and the lift coefficient increases considerably for all angles of attack. Fig. 17(c) demonstrates that, for all angles of attack greater than zero, the lift to drag ratio increases with increasing the top surface temperature of the wing. A lift enhancement of 70% and a drag reduction of 48% can be seen in Fig. 17(d) for angles of attack of 6 and 2 degrees, respectively.

Fig. 18(a) demonstrates that for MH 20, the drag coefficient is decreasing with heating the top surface of the wing for the angles of attack

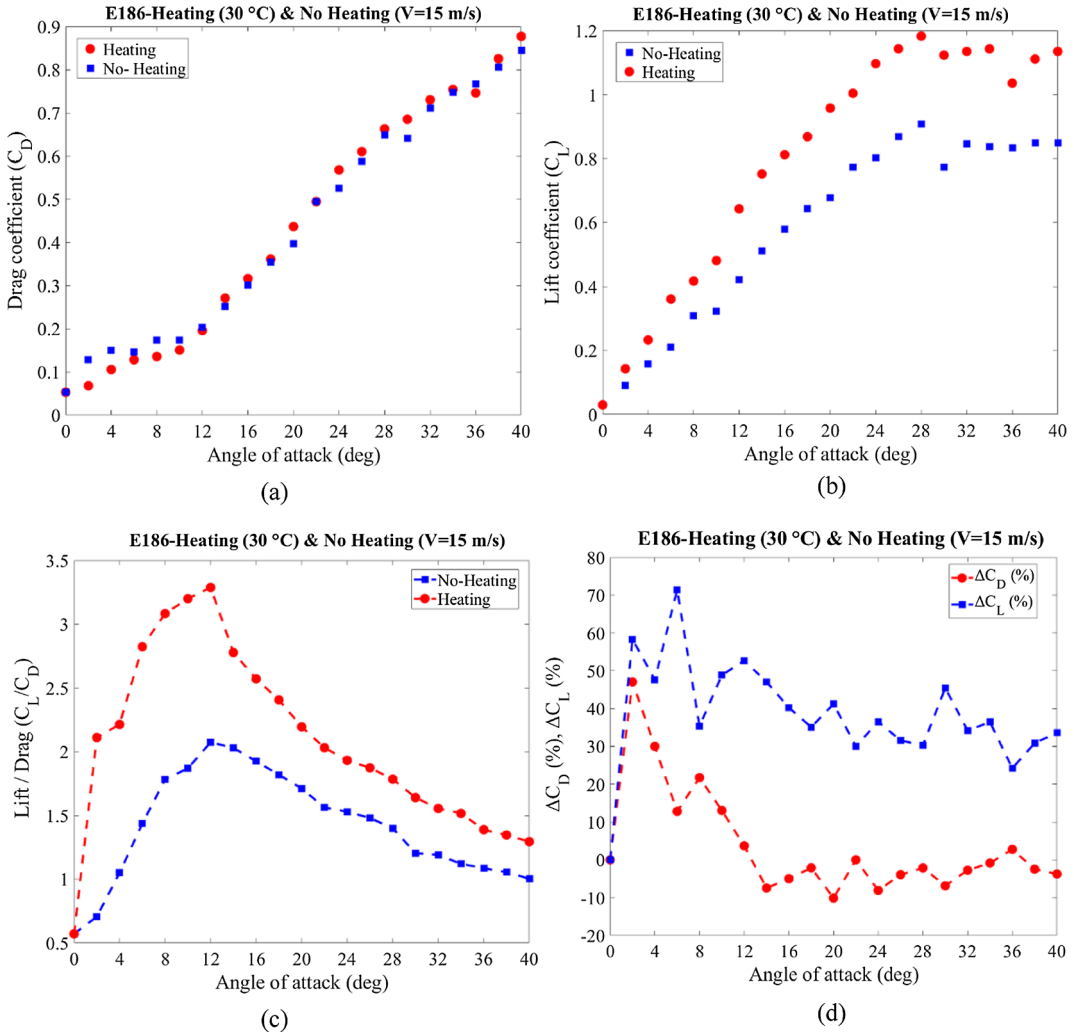

Fig. 17. View of (a) drag coefficient, (b) lift coefficient, (c) lift to drag, and (d) relative changes (percentages) of the lift and drag coefficients versus angle of attack of E186 for heating and no heating conditions in the wind speed of 15 m/s.

less than 16 degrees. It can be found from Fig. 18(b) that the lift coefficient for the top-heated wing increases until the stall angle of attack of 30 degrees. A considerable enhancement in the lift to drag ratio can be seen in Fig. 18(c) for angles of attack up to 18 degrees. For angles of attack more than 18 degrees, the lift to drag ratio does not change with heating the top surface of the wing. It is shown from Fig. 18(d) that a drag reduction of 60% and lift enhancement of 25% can be achieved for a top-heated wing at an angle of attack of 2 and 4 degrees, respectively.

In Fig. 19, the lift to drag ratio enhancement in top heating wings compared to no heating condition is shown versus angle of attack for different studied airfoils. The results indicate that E186 and GOE 174 have the highest performance compared the other airfoils. E186 is also showing a lift to drag ratio enhancement of almost two times of other airfoils for higher angles of attack that this can be explained due to the geometrical characteristics of this reflexed airfoil. Moreover, It is apparent that the highest enhancement percentage of the lift to drag ratios are generally achieved in the lower angles of attack. For angles of attack more than 14 degrees, it can be seen the lift to drag ratio enhancement decreases for all the airfoils and has almost a constant value. It can be concluded that for higher values of angles of attack, with heating the top surface of the wings and increasing the angle of attack, the enhancement in the lift to drag ratio is changing slightly.

7. Conclusions

Thermal analysis of temperature differences identified in natural flyers has been carried out to better understand the impact it can have on flight efficiency. Experimental studies were performed on black and white wings as well as aluminum plates to study the effects of their emissivity on their surface temperature. It was shown that black colors can get over 50% hotter than white, and due to the different conductivity coefficients, the birds' wings reach higher temperatures than the same colored aluminum plates. These effects seem to play a major role in birds' efficiency. Through the application of such a concept, a study was performed on heated top surfaces of various airfoils. It has been found that at low angles of attack, the overall efficiency can be substantially increased through the application of a thin, heated layer on the top surface of the airfoil.

Declaration of Competing Interest

The author(s) declared no potential conflicts of interest with respect to the research, authorship, and/or publication of this article.

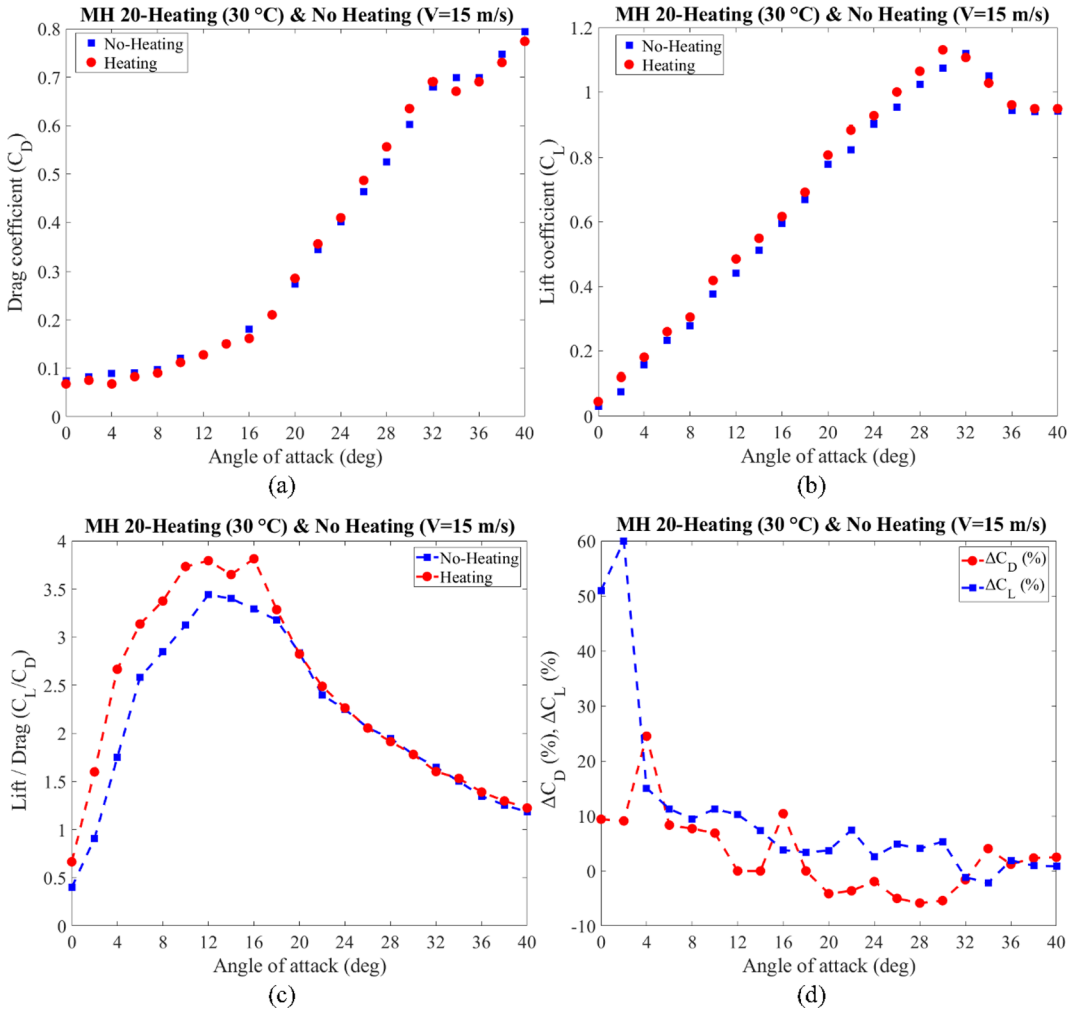

Fig. 18. View of (a) drag coefficient, (b) lift coefficient, (c) lift to drag, and (d) relative changes (percentages) of the lift and drag coefficients versus angle of attack of MH20 for heating and no heating conditions in the wind speed of 15 m/s.

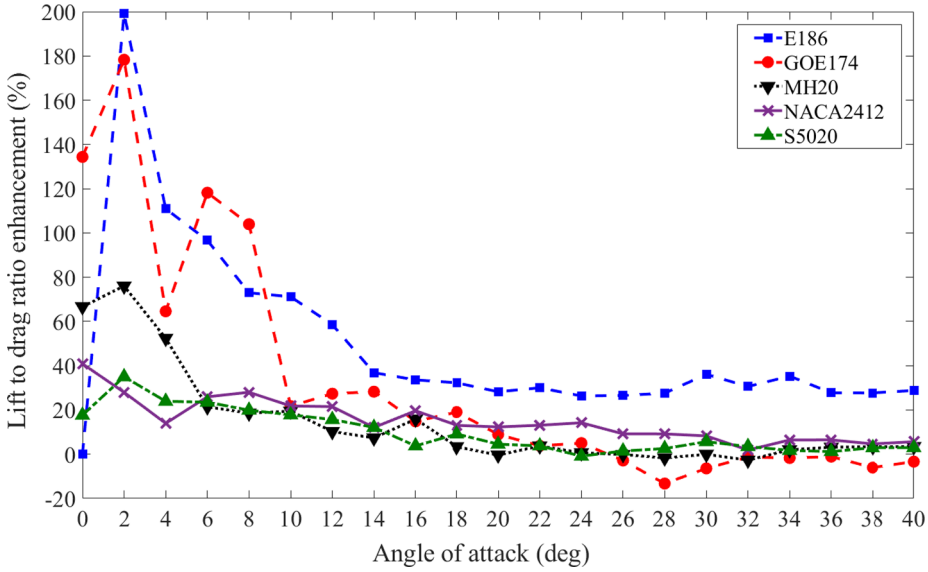

Fig. 19. Lift to drag ratio enhancement percentage versus angle of attack.

Acknowledgment

The authors Mostafa Hassanalian and Victoria Pellerito gratefully acknowledge the financial support from the National Science Foundation. A part of this study was supported by the INTENSE REU program. The INTENSE REU is funded by the National Science Foundation (NSF) Division of Engineering Education and Centers (EEC), United States, award #1757793. The project is led at New Mexico Tech by PI Dr. Michael Hargather and Co-PI Dr. Mostafa Hassanalian.

References

[1] M. Hassanalian, A. Abdelkefi, Classifications, applications, and design challenges of drones: a review, Prog. Aerosp. Sci. 91 (2017) 99–131.
[2] M. Hassanalian, D. Rice, A. Abdelkefi, Evolution of space drones for planetary exploration: a review, Prog. Aerosp. Sci. 97 (2018) 61–105.
[3] M. Hassanalian, A. Quintana, A. Abdelkefi, Morphing and growing micro unmanned air vehicle: sizing process and stability, Aerosp. Sci. Technol. 78 (2018) 130–146.
[4] M. Hassanalian, A. Abdelkefi, Design, manufacturing, and flight testing of a fixed wing micro air vehicle with Zimmerman planform, Meccanica 52 (6) (2017) 1265–1282.
[5] A. Mirzaeinia, M. Hassanalian, K. Lee, M. Mirzaeinia, Performance Enhancement and Load Balancing of Swarming Drones through Position Reconfiguration. In: AIAA Aviation 2019 Forum, Dallas, TX, 17-21 June 2019.
[6] M. Hassanalian, M. Radmanesh, A. Sedaghat, Increasing flight endurance of MAVs using multiple quantum well solar cells, Int. J. Aeronaut. Space Sci. 15 (2014) 212–217.
[7] D.M. Bushnell, K.J. Moore, Drag reduction in nature, Annu. Rev. Fluid Mech. 23 (1) (1991) 65–79.
[8] M. Hassanalian, H. Abdelmoula, S. Mohammadi, S. Bakhtiyarov, J. Goerlich, U. Javed, Insight into the Thermal Effects of Aquatic Animal Colors on their Skin Friction Drag, in: AIAA Aviation 2019 Forum, Dallas, TX, 17-21 June 2019, 2019.
[9] M. Hassanalian, H. Abdelmoula, S.B. Ayed, A. Abdelkefi, Thermal impact of migrating birds' wing color on their flight performance: possibility of new generation of biologically inspired drones, J. Therm. Biol 66 (2017) 27–32.
[10] M. Hassanalian, S.B. Ayed, M. Ali, P. Houde, C. Hocut, A. Abdelkefi, Insights on the thermal impacts of wing colorization of migrating birds on their skin friction drag and the choice of their flight route, J. Therm. Biol 72 (2018) 81–93.
[11] M. Hassanalian, G. Throneberry, M. Ali, S.B. Ayed, A. Abdelkefi, Role of wing color and seasonal changes in ambient temperature and solar irradiation on predicted flight efficiency of the Albatross, J. Therm. Biol 71 (2018) 112–122.
[12] K.F. Stetson, R.L. Kimmel, Surface temperature effects on boundary-layer transition, AIAA J. 30 (11) (1992) 2782–2783.
[13] T. Nonweiler, H.Y. Wong, S.R. Aggarwal, The role of heat conduction in leading edge heating, Ingenieur-Archiv 40 (2) (1971) 107–117.
[14] Z.X. Yuan, W.Q. Tao, X.T. Yan, Experimental study on heat transfer in ducts with winglet disturbances, Heat Transf. Eng. 24 (2) (2003) 76–84.
[15] F. Xie, Z.Y. Ye, The simulation of the airship flow field with injection channel for the drag reduction, Eng. Mech. V27 (2010).
[16] J. Hua, F. Kong, H.H. Liu, Unsteady thermodynamic computational fluid dynamics simulations of aircraft wing anti-icing operation, J. Aircraft 44 (4) (2007) 1113–1117.
[17] R. Kamboj, S. Dhingra, G. Singh, CFD simulation of heat transfer enhancement by plain and curved winglet type vertex generators with punched holes, Int. J. Eng. Res. General Sci. 2 (4) (2014) 2091–2730.
[18] T.F. Gelder, J.P. Lewis, Comparison of heat transfer from airfoil in natural and simulated icing conditions, in: Lewis Flight Propulsion Laboratory Cleveland, NACA Technical Note 2480, Ohio, 1951.
[19] V. Dragan, Influences of surface temperature on a low camber airfoil aerodynamic performances, INCAS Bull. 8 (1) (2016) 49.
[20] M. Brooke, Albatrosses and petrels across the world, Oxford University Press, 2004.
[21] P. Jouventin, H. Weimerskirch, Satellite tracking of wandering albatrosses, Nature 343 (6260) (1990) 746.
[22] J. Warham, The behaviour, population biology and physiology of the petrels, Academic Press, 1996.
[23] G. Sachs, J. Traugott, A.P. Nesterova, G. Dell'Omo, F. Kümmeth, W. Heidrich, A.L. Vyssotski, F. Bonadonna, Flying at no mechanical energy cost: disclosing the secret of wandering albatrosses, PLoS ONE 7 (9) (2012) e41449.
[24] P. Catry, R.A. Phillips, J.P. Croxall, Sustained fast travel by a gray-headed albatross (Thalassarche chrysostoma) riding an Antarctic storm, Auk 121 (4) (2004) 1208–1213.
[25] C.J. Pennycuick, The flight of petrels and albatrosses (Procellariiformes), observed in South Georgia and its vicinity, Philos. Trans. Royal Soc. Lond. B: Biol. Sci. 300 (1098) (1982) 75–106.
[26] P.L. Richardson, How do albatrosses fly around the world without flapping their wings? Prog. Oceanogr. 88 (1) (2011) 46–58.